



Chemical characteristics of PM_{2.5} during dust storms and air pollution events in Chengdu, China

Qiyuan Wang^{a,b}, Junji Cao^{b,c,*}, Zhenxing Shen^a, Jun Tao^d, Shun Xiao^{b,e,f}, Lei Luo^g, Qingyang He^b, Xinying Tang^g

^a Department of Environmental Science and Engineering, Xi'an Jiaotong University, Xi'an 710049, China

^b Key Lab of Aerosol Science & Technology, SKLLQG, Institute of Earth Environment, Chinese Academy of Sciences, Xi'an 710075, China

^c Institute of Global Environmental Change, Xi'an Jiaotong University, Xi'an 710049, China

^d South China Institute of Environmental Sciences, SEPA, Guangzhou 510655, China

^e Meteorological Bureau of Baoji Municipality, Baoji 721006, China

^f Climate Center of Shaanxi Meteorological Bureau, Xi'an 710014, China

^g Institute of Plateau Meteorology, CMA, Chengdu, Chengdu 610071, China

ARTICLE INFO

Article history:

Received 23 December 2011

Received in revised form 19 June 2012

Accepted 13 August 2012

Keywords:

PM_{2.5}

Chemical species

Pollution events

Mass balance

ABSTRACT

Daily fine particulate (PM_{2.5}) samples were collected in Chengdu from April 2009 to February 2010 to investigate their chemical profiles during dust storms (DSs) and several types of pollution events, including haze (HDs), biomass burning (BBs), and fireworks displays (FDs). The highest PM_{2.5} mass concentrations were found during DSs (283.3 μg/m³), followed by FDs (212.7 μg/m³), HDs (187.3 μg/m³), and BBs (130.1 μg/m³). The concentrations of most elements were elevated during DSs and pollution events, except for BBs. Secondary inorganic ions (NO₃⁻, SO₄²⁻, and NH₄⁺) were enriched during HDs, while PM_{2.5} from BBs showed high K⁺ but low SO₄²⁻. FDs caused increases in K⁺ and enrichment in SO₄²⁻. Ca²⁺ was abundant in DS samples. Ion-balance calculations indicated that PM_{2.5} from HDs and FDs was more acidic than on normal days, but DS and BB particles were alkaline. The highest organic carbon (OC) concentration was 26.1 μg/m³ during FDs, followed by BBs (23.6 μg/m³), HDs (19.6 μg/m³), and DSs (18.8 μg/m³). In contrast, elemental carbon (EC) concentration was more abundant during HDs (10.6 μg/m³) and FDs (9.5 μg/m³) than during BBs (6.2 μg/m³) and DSs (6.0 μg/m³). The highest OC/EC ratios were obtained during BBs, with the lowest during HDs. SO₄²⁻/K⁺ and TCA/SO₄²⁻ ratios proved to be effective indicators for differentiating pollution events. Mass balance showed that organic matter, SO₄²⁻, and NO₃⁻ were the dominant chemical components during pollution events, while soil dust was dominant during DSs.

© 2012 Chinese Society of Particuology and Institute of Process Engineering, Chinese Academy of Sciences. Published by Elsevier B.V. All rights reserved.

1. Introduction

Ambient air pollution is associated with a wide range of potential health effects in human beings (de Kok, Driess, Hogervorst, & Briedé, 2006; Ning & Sioutas, 2010; Pope et al., 2002). Haze usually occurs when sunlight encounters many tiny pollution particles in ambient air that can absorb or scatter light (Husar & Holloway, 1984). Over the past several decades, large quantities of pollutants have been unavoidably emitted into the atmosphere with economic expansion in China (Tie et al., 2006). Che et al. (2009) pointed out an increasing trend toward haze occurrences in eastern and

southwestern cities in China. Most of this haze results from excessive particulate matter (PM) emitted by anthropogenic sources and particles produced by gas-to-particle conversion (Watson, 2002). Dust storm events are another atmospheric phenomenon, and the primary origins of dust events in eastern Asia are in Mongolia and northern China (Wang, Yuan, & Shang, 2006). When dust storms occur, air quality, transportation, and even people's lives are noticeably affected (Wang et al., 2006). Smoke aerosols released from biomass burning are complex chemical mixtures of organics, inorganics, and gases which may increase the risk of bronchial asthma in children who live near areas where biomass is burned (Torrigio et al., 2000). Fireworks displays are common during traditional Chinese Spring Festivals and Lantern Festivals. They can also cause serious air pollution, including high levels of sulfates, nitrates, and trace metals, which can pose a threat to human health (Shen et al., 2009; Wang, Zhuang, Xu, & An, 2007).

* Corresponding author at: Key Lab of Aerosol Science & Technology, SKLLQG, Institute of Earth Environment, Chinese Academy of Sciences, Xi'an 710075, China. Tel.: +86 29 8832 6488; fax: +86 29 8832 0456.

E-mail address: cao@loess.llqg.ac.cn (J. Cao).

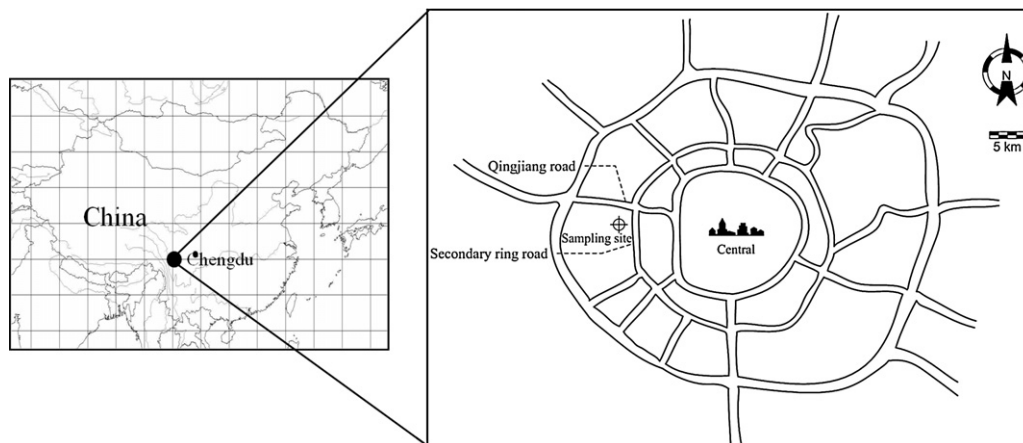


Fig. 1. Location of sampling site.

Chengdu (30.67°N, 104.06°E, 500 m above sea level), the largest city in southwestern China, is situated in the midwestern portion of the Sichuan basin, which has a population of ~11 million and an area of ~12,000 km². With increasing energy consumption and rising numbers of motor vehicles, PM pollution has become the primary environmental problem in Chengdu (Henriksson et al., 2011; Shi et al., 2011). During recent decades, the numbers of events in which the visual range was <10 km per year in Chengdu increased dramatically from 169 days in 1973 to 339 days per year in 2007 (Chang, Song, & Liu, 2009).

Because of the potential effects of pollution episodes on the environment and on human health, several studies have focused on various pollution events (Kim et al., 2003; Lee, Kim, & Kim, 2006; Shen et al., 2009). However, few studies have considered the chemical compositions of pollution events simultaneously, especially in Chengdu. In this study, trace elements, water-soluble ions, and carbonaceous species were investigated to reveal the chemical profile of PM_{2.5} during dust storms and pollution events.

2. Methodology

2.1. Sample collection

Sampling was conducted on the rooftop (~20 m above ground level) of the Institute of Plateau Meteorology, Chengdu. The site is located in the western part of downtown Chengdu in a residential/commercial neighborhood (Fig. 1). Intensive measurements were carried out during four seasons: in spring (April 18 to May 18), summer (July 5 to August 6), and autumn (October 26 to November 26) in 2009, and in winter (February 8 to 28) in 2010.

Twenty-four hour PM_{2.5} samples were collected daily from 1000 local standard time (LST) to 1000 LST the next day using two battery-powered mini-volume samplers (Airmetrics, Oregon, USA) with a flow rate of 5 L/min. One set was collected onto 47-mm Whatman quartz microfibre filters (QM/A; Whatman, Middlesex, UK) for water-soluble ion, organic carbon (OC), and elemental carbon (EC) analyses; the other set was collected onto 47-mm Teflon filters (Whatman Limited, Maidstone, UK) for elemental analysis. A total of 115 pairs of samples were obtained, including 35 pairs on normal days (NDs), 68 pairs on hazy days (HDs), 2 pairs during dust storms (DSs), 8 pairs on biomass-burning days (BBs), and 2 pairs during fireworks displays (FDs). Among the 68 HD samples, 14 were collected in spring, 20 in summer, 23 in autumn, and 11 in winter. DS and BB samples were collected in spring; FD samples were collected during the Chinese Spring Festival and Lantern

Festival. After sampling, filters were placed in plastic cassettes and stored in a refrigerator at 4 °C until analysis.

2.2. Mass and chemical analyses

PM_{2.5} samples were equilibrated using controlled temperature (20–23 °C) and relative humidity (35–45%) desiccators for 24 h before and after sampling and then weighed on a Sartorius MC5 electronic microbalance with ±1 µg sensitivity (Sartorius, Göttingen, Germany). Samples were stored under airtight conditions in a refrigerator at approximately 4 °C before chemical analysis to prevent evaporation of volatilized components.

As shown in Table 1, 13 elements were determined by energy-dispersive X-ray fluorescence (ED-XRF) spectrometry (Cao et al., 2012) (Epsilon 5 ED-XRF, PANalytical B.V., The Netherlands). These elements included Al, S, Cr, Mn, Ti, Fe, Zn, As, Br, Sr, Ba, Pb, and Cu. Each sample was analyzed for one-half hour, and a field blank consisting of a Teflon filter sample was also analyzed to evaluate analytical bias.

Water-soluble ions were determined by ion chromatography (Chow & Watson, 1999) (IC, Dionex 600, Dionex, Sunnyvale, CA). Cations, including NH₄⁺, K⁺, Mg²⁺, and Ca²⁺, were determined using a CS12A column (Dionex) with 20 mM methanesulfonic acid eluent. Anions, including F⁻, Cl⁻, NO₃⁻, and SO₄²⁻, were analyzed using an AS11-HC column (Dionex) with 20 mM potassium hydroxide (KOH) eluent. Detection limits were 4.0 mg/L for NH₄⁺, 10.0 mg/L for K⁺, Mg²⁺, and Ca²⁺, 0.5 mg/L for Cl⁻ and F⁻, 20 mg/L for SO₄²⁻, and 15 mg/L for NO₃⁻. Standard reference materials produced by the National Research Center for Certified Reference Materials in China were analyzed for quality assurance purposes.

Carbonaceous species (OC and EC) were analyzed using the thermal/optical reflectance (TOR) method (Chow et al., 2007, 2011) on a DRI Model 2001 Thermal/Optical Carbon Analyzer (Atmoslytic Inc., Calabasas, CA, USA). The IMPROVE-A protocol (Chow et al., 2007) produces four OC fractions (OC1, OC2, OC3, and OC4 at 140 °C, 280 °C, 480 °C, and 580 °C respectively in a 100% helium (He) atmosphere); a pyrolyzed carbon fraction (OP, determined when reflected or transmitted laser light attained its original intensity after oxygen (O₂) was added to the analysis atmosphere); and three EC fractions (EC1, EC2, and EC3 in a 98% He/2% O₂ atmosphere at 580 °C, 740 °C, and 840 °C respectively). OC was defined as OC1 + OC2 + OC3 + OC4 + OP and EC as EC1 + EC2 + EC3 – OP. The analyzer was calibrated daily with known quantities of methane (CH₄) (Cao et al., 2003; Chow et al., 2011).

Table 1
Chemical species and analytical methods.

Parameters	Contents	Analytical method	QA/QC
Elements	Al, S, Cr, Mn, Ti, Fe, Zn, As, Br, Sr, Ba, Pb, and Cu	Energy dispersive X-ray fluorescence	The ED-XRF spectrometer was calibrated with thin-film standards bias.
Water-soluble ions	NH ₄ ⁺ , K ⁺ , Mg ²⁺ , Ca ²⁺ , F ⁻ , Cl ⁻ , NO ₃ ⁻ , and SO ₄ ²⁻	Ion chromatography	Standard reference materials produced by the National Research Center for Certified Reference Materials in China were analyzed for quality assurance purposes. The analyzer was calibrated daily with known quantities of methane (CH ₄).
Carbonaceous species	Organic carbon and elemental carbon	Thermal/optical reflectance (TOR)	

QA/QC: quality assurance/quality control.

2.3. Meteorological data

Meteorological data, including ambient temperature, relative humidity (RH), wind speed (WS), and atmospheric pressure, were collected from Weather Underground (www.wunderground.com).

3. Results and discussion

3.1. PM_{2.5} mass concentrations during four PM events

The mass concentrations of PM_{2.5} and the meteorological conditions during NDs, DSs, and pollution events are summarized in Table 2. The average mass concentrations of PM_{2.5} were 283.3, 212.7, 187.3, and 130.1 μg/m³ during DSs, FDs, HDs, and BBs respectively, which exceeded the Chinese government's recently issued 24-h PM_{2.5} standard of 75 μg/m³ by a factor of approximately two to four (http://www.chinadaily.com.cn/china/2012-03/03/content_14745568.htm). The average PM_{2.5} mass concentration during DSs was 3.6 times higher than that during NDs, while during HDs, BBs, and FDs it was 1.7–2.7 times higher than during NDs. Compared with PM_{2.5} concentrations in other cities in China, the average PM_{2.5} concentrations during DSs and pollution events in Chengdu were higher than the values of 57.9 μg/m³ observed in Shanghai (Ye et al., 2003), 103.0 μg/m³ in Guangzhou (Andreae et al., 2008), and 44.3 μg/m³ in Fuzhou (Xu et al., 2012), thus suggesting a very serious potential health concern in the Chengdu urban atmosphere.

HDs were the most commonly observed pollution events during the sampling periods. As shown in Table 2, HDs were more strongly associated with lower wind speed and higher relative humidity than NDs. Low wind speed had a negative effect on atmospheric convection and diffusion, while high RH can enhance the growth

of hygroscopic particles (i.e., sulfates and nitrates) which scatter more light (Watson, 2002).

3.2. Elemental compositions during four PM events

The average concentrations of the elements detected in PM_{2.5} during NDs, DSs, and pollution events are summarized in Table 3. The total concentrations of all measured elements were 5.8, 36.0, 13.0, 7.4, and 22.0 μg/m³, accounting for 7.5%, 12.7%, 6.9%, 5.7%, and 10.4% of PM_{2.5} mass during NDs, DSs, HDs, BBs, and FDs respectively. S, Fe, Al, and Zn were the dominant elements during NDs, accounting for ~92% of all measured elements. The concentrations of the typical dust elements Al (15.9 μg/m³), Fe (13.3 μg/m³), Ti (1.1 μg/m³), and Mn (0.4 μg/m³) were higher during DSs than during NDs and other pollution events, and the sum of these elements accounted for ~85% of all measured elements. The concentrations of these dust elements were higher than in aerosol samples of the same size fraction collected in the Horqin sandy land in northeastern China (Shen et al., 2007), where the average concentrations of Al, Fe, Ti, and Mn were 3.8, 3.0, 0.2, and 0.1 μg/m³ respectively. It is noteworthy that the levels of some pollution elements (e.g., Zn, Br, Pb, Cu, and As) during DSs were 1.6–2.6 times higher than those during NDs, which indicates that the presence of these elements might be partially due to long-range transport of dust particles.

Other elements occurring during HDs were S, Fe, Zn, Al, and Pb in decreasing order of concentration, with levels of the remaining elements being lower than 0.2 μg/m³. S, Fe, Zn, and Al together accounted for ~93% of all measured elements. The concentrations of S, Pb, Cu, Br, and As during HDs were 2.0–4.2 times higher than during NDs. High S concentrations in HD samples signified the presence of coal combustion. This can be further proved by comparing the S/Al ratios in fugitive dust profile samples from the Loess Plateau (Cao et al., 2008) with those in PM_{2.5} samples from

Table 2
Average PM_{2.5} mass concentrations and meteorological conditions during normal days, dust storms, and pollution events.

Events		PM _{2.5} (μg/m ³)	Temperature (°C)	Humidity (%)	Pressure (hPa)	Wind speed (m/s)
NDs (n = 35)	Average	77.9	18.4	67.2	1013.9	2.2
	S.D.	19.5	7.4	14.4	9.9	1.0
DSs (n = 2)	Average	283.3	20.6	48.5	1018.9	1.1
	S.D.	24.4	0.1	1.6	0.4	0.2
HDs (n = 68)	Average	187.3	17.5	73.4	1013.0	1.1
	S.D.	105.5	7.6	7.9	9.0	0.6
BBs (n = 8)	Average	130.1	22.3	65.4	1008.9	1.9
	S.D.	34.0	1.8	15.0	3.8	1.0
FDs (n = 2)	Average	212.7	11.4	68	1012.7	1.4
	S.D.	105.8	7.7	4.2	8.5	0.3

NDs: normal days; DSs: dust storms; HDs: haze days; BBs: biomass-burning days; FDs: fireworks displays; and S.D.: standard deviation.

Table 3Concentrations of elements in PM_{2.5} during normal days, dust storms, and pollution events (unit in $\mu\text{g}/\text{m}^3$).

	NDs (n=35)		DSs (n=2)		HDs (n=68)		BBs (n=8)		FDs (n=2)	
	Average	S.D.	Average	S.D.	Average	S.D.	Average	S.D.	Average	S.D.
S	3.28	1.07	3.64	0.92	9.36	3.93	4.63	2.89	13.54	7.23
Fe	0.89	0.69	13.30	1.16	1.28	0.81	1.14	0.42	0.82	0.69
Al	0.80	0.97	15.87	2.58	0.73	0.87	0.82	0.62	2.21	0.31
Zn	0.40	0.24	1.05	0.52	0.77	0.44	0.36	0.11	1.07	1.23
Pb	0.17	0.06	0.28	0.14	0.34	0.15	0.17	0.08	1.25	0.52
Ti	0.08	0.06	1.09	0.11	0.11	0.07	0.09	0.04	0.19	0.07
Mn	0.07	0.03	0.40	0.00	0.12	0.06	0.07	0.02	0.11	0.10
Sr	0.05	0.05	0.00	0.01	0.06	0.05	0.00	0.00	0.46	0.02
Ba	0.04	0.04	0.22	0.02	0.06	0.07	0.01	0.02	2.03	0.52
Cu	0.03	0.01	0.06	0.02	0.06	0.03	0.03	0.01	0.27	0.09
Br	0.01	0.01	0.03	0.01	0.06	0.04	0.02	0.02	0.03	0.05
As	0.02	0.01	0.03	0.01	0.04	0.03	0.00	0.01	0.05	0.03
Cr	0.01	0.00	0.03	0.00	0.02	0.01	0.01	0.01	0.01	0.01

NDs: normal days; DSs: dust storms; HDs: haze days; BBs: biomass-burning days; FDs: fireworks displays; and S.D.: standard deviation.

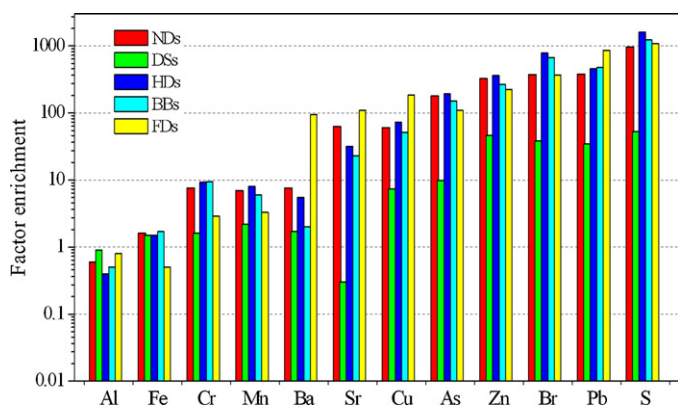
Chengdu, where there was no fugitive dust profile. The S/Al ratio was 12.9 for HDs, which was over three orders of magnitude greater than the S/Al ratio of 0.01 for fugitive dust profile samples.

Similar to the ND and HD samples, S, Fe, Al, and Zn during BBs together accounted for ~94% of all measured elements. However, the dominant elements changed to S, Al, Ba, and Pb during FDs, a group which together accounted for ~86% of all measured elements. The concentrations of most elements during BBs were comparable to or lower than those during NDs. However, the concentrations of Pb, Sr, Cu, and Ba during FDs were respectively 7.3, 8.4, 10.1, and 52.1 times greater than those during NDs, which was indicative of the presence of highly toxic metals in the fireworks. Wang et al. (2007) also found enhanced concentrations of Pb, Sr, Cu, and Ba during the lantern festival in Beijing during 2006.

To distinguish between elements originating from natural and anthropogenic emissions, enrichment factors (EFs) were calculated for the measured elements during different PM episodes. In this study, EFs were calculated using Ti as the reference element (Cao, Shen, Chow, Qi, & Watson, 2009). The equation used for calculating the EFs is:

$$EF = \frac{[C_X/C_{Ti}]_{\text{aerosol}}}{[C_X/C_{Ti}]_{\text{crust}}}, \quad (1)$$

where $[C_X/C_{Ti}]_{\text{aerosol}}$ is the average concentration ratio of C_X to C_{Ti} in the aerosol sample and $[C_X/C_{Ti}]_{\text{crust}}$ is the concentration ratio of C_X to C_{Ti} in the crust. As shown in Fig. 2, the EF values for Al, Fe, Cr, and Mn for NDs, DSs, and pollution events were in the 1–10 range, suggesting that they came mainly from crustal sources. However, much higher EFs, ranging from 35 to 1603, were found for Zn, Br, Pb,

**Fig. 2.** Enrichment factors of the elements during normal days (NDs), dust storms (DSs), haze days (HDs), biomass-burning days (BBs), and fireworks displays (FDs).

and S, indicating that for these elements, anthropogenic emissions were predominant. Previous studies have indicated that Cu, Zn, Br, and Pb can often serve as markers associated with traffic sources (Xu et al., 2012), while S and As in atmospheric particles are coal combustion indicators (Cao et al., 2009; Tian et al., 2010). The EF values for Cu, As, Zn, Br, Pb, and S during HDs (73–1603) were much higher than those during NDs (60–951), indicating that vehicular emissions and coal burning enhanced these elements during HDs. The EF values for Ba, Sr, Cu, and Pb during FDs were 94, 109, 185, and 858 respectively, which indicated that fireworks enhanced these elements.

3.3. Ionic characteristics during four PM events

The average concentrations and standard deviations of the major water-soluble ions in PM_{2.5} during NDs, DSs, and pollution events are summarized in Table 4. The concentrations of total water-soluble ions were 32.8, 36.6, 87.6, 44.9, and 128.4 $\mu\text{g}/\text{m}^3$, accounting for 42.0%, 12.9%, 46.7%, 34.5%, and 60.3% of PM_{2.5} mass during NDs, DSs, HDs, BBs, and FDs respectively. Elevated Ca^{2+} , making up 33.3% of total ions, was found during DSs, which was consistent with other studies (Shen et al., 2011). However, the concentrations of secondary inorganic ions during DSs were at the lowest levels observed for all PM events and surprisingly even lower than during NDs. A similar result was also found by Shen et al. (2009) for Xi'an dust storms.

During HDs, approximately 84.6% of the total measured ions was attributed to secondary inorganic ions (e.g., SO_4^{2-} , NO_3^- , and NH_4^+), and the concentrations of these were 2.8–4.9 times higher than for NDs. In an urban atmosphere, aerosol SO_4^{2-} and NO_3^- are formed mainly by conversion of gaseous precursors. The results showed that unfavorable meteorological factors (e.g., low wind speed and high RH) during HDs could enhance heterogeneous conversion efficiency. Because coal burning is the major source of As, a strong relationship ($r=0.72$) between As and SO_4^{2-} suggested that coal burning was the major source of sulfate during HDs.

Similarly to the results for the HD samples, SO_4^{2-} , NO_3^- , and NH_4^+ were the dominant ions during BBs, accounting for 67.2% of total ions. The chemical profiles for BBs were strongly enriched in K^+ , which made up 11.1% of the total ions; these results are consistent with those of BB studies conducted in Xi'an by Shen et al. (2009). Compared with other PM events, the mass concentrations of ions during FDs could be ranked in the order $\text{SO}_4^{2-} > \text{K}^+ > \text{NO}_3^- > \text{Cl}^- > \text{NH}_4^+ > \text{Mg}^{2+} > \text{F}^- > \text{Ca}^{2+}$. This was in contrast with the results reported by Shen et al. (2009), in which NO_3^- was the largest contributor to PM_{2.5} during FDs in Xi'an. Potassium

Table 4
Concentrations of water-soluble ions in PM_{2.5} during normal days, dust storms, and pollution events (unit in $\mu\text{g}/\text{m}^3$).

	NDs (n = 35)		DSs (n = 2)		HDs (n = 68)		BBs (n = 8)		FDs (n = 2)	
	Average	S.D.	Average	S.D.	Average	S.D.	Average	S.D.	Average	S.D.
SO ₄ ²⁻	14.01	5.80	12.51	2.49	39.03	20.47	15.18	9.46	60.70	35.92
NO ₃ ⁻	7.45	2.68	6.28	2.86	22.74	13.92	9.91	5.36	18.15	9.26
Cl ⁻	1.83	1.30	2.94	1.66	4.34	3.19	3.02	2.14	13.00	4.95
F ⁻	0.16	0.11	0.32	0.13	0.25	0.20	0.14	0.04	0.45	0.07
NH ₄ ⁺	2.49	2.01	0.10	0.08	12.33	7.59	5.04	4.38	10.35	7.28
Ca ²⁺	4.79	3.35	11.91	0.22	4.69	3.22	5.04	1.30	0.20	0.14
K ⁺	1.71	0.81	1.95	0.12	3.78	1.92	4.97	2.08	23.40	8.91
Mg ²⁺	0.33	0.20	0.58	0.00	0.40	0.28	1.56	0.60	2.10	0.57

NDs: normal days; DSs: dust storms; HDs: haze days; BBs: biomass-burning days; FDs: fireworks displays; and S.D.: standard deviation.

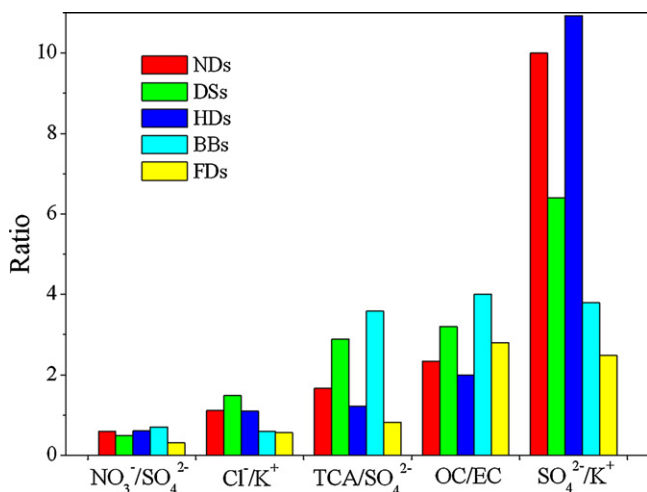


Fig. 3. Ratios of chemical species in PM_{2.5} during normal days (NDs), dust storms (DSs), haze days (HDs), biomass-burning days (BBs), and fireworks displays (FDs).

(K) is one of the major components of fireworks because approximately 74% of black powder consists of KNO₃, which provides the main oxidant for burning (Vecchi et al., 2008). Elevated K⁺, accounting for 18.2% of total ions, was observed during FDs.

To investigate further the characteristics of PM_{2.5} during DSs and pollution events, several ionic ratios were calculated and are compared in Fig. 3. Several studies have suggested that the NO₃⁻/SO₄²⁻ ratio can be used to evaluate the influence of mobile versus stationary pollution sources (Arimoto et al., 1996). However, the NO₃⁻/SO₄²⁻ ratio has been found to depend not only on the composition of the primary emissions, but also strongly on the occurrence of chemical reactions. Average NO₃⁻/SO₄²⁻ ratios were low during DSs (0.49) and FDs (0.31), whereas these ratios increased to 0.59, 0.60, and 0.70 during NDs, HDs, and BBs respectively, indicating the dominant contribution of coal burning to PM_{2.5} in Chengdu. The NO₃⁻/SO₄²⁻ ratios found in this study were lower than values reported for Beijing (0.71) (Wang et al., 2005) and Guangzhou (0.79) (Tan et al., 2009), where traffic densities are

high. The average SO₄²⁻/K⁺ ratio was 3.8 for BBs and 2.5 for FDs, with much higher values for DSs (6.4), NDs (10.0), and HDs (10.9). A similar pattern was also found for the Cl⁻/K⁺ ratio. Low SO₄²⁻/K⁺ and Cl⁻/K⁺ ratios may be useful for distinguishing BBs and FDs from other PM events.

Ion-balance calculations can be used to study the acid–base balance of aerosol particles (Shen et al., 2007, 2008, 2010, 2011). The cation and anion microequivalents for PM_{2.5} samples from various episodes were calculated as follows:

$$C(\text{cation microequivalents}) = \text{Na}^+/23 + \text{NH}_4^+/18 + \text{K}^+/39 + \text{Mg}^{2+}/12 + \text{Ca}^{2+}/20, \quad (2)$$

$$A(\text{anion microequivalents}) = \text{F}^-/19 + \text{Cl}^-/35.5 + \text{NO}_3^-/62 + \text{SO}_4^{2-}/48 \quad (3)$$

Fig. 4(a) shows a high correlation ($r=0.95$) between the cation and anion equivalents among all PM_{2.5} samples, with a regression slope of 1.54 ± 0.04 , which was indicative of a cation deficiency. Although the ND samples were dispersed around the 1:1 anion:cation (A:C) line, the A/C ratio was close to unity (Fig. 4(b)). Approximately 82% of the samples from HDs and all the samples from FDs fell above the 1:1 A:C line (Fig. 4(c)), which implied that these samples were acidic. Average A/C ratios for HDs (1.2) and FDs (1.4) were higher than for NDs (1.1), which was indicative of more acidic conditions during pollution events. The relatively high A/C ratios for HDs and HFs might be caused by high concentrations of SO₄²⁻ and NO₃⁻. The ion balances for DS and BB samples were positioned below the A:C unity line (Fig. 4(d)), which indicated that these samples were alkaline.

3.4. Carbonaceous species during four PM events

Table 5 shows the distribution of carbonaceous species for NDs, DSs, and pollution events. The average OC concentrations were 18.8, 19.6, 23.6, and 26.1 $\mu\text{g}/\text{m}^3$, accounting for 6.6%, 10.5%, 18.1%, and 12.2% of PM_{2.5} mass for DSs, HDs, BBs, and FDs respectively. The OC concentration during DSs was 2.0 times higher than that

Table 5
Distribution of carbonaceous species (unit in $\mu\text{g}/\text{m}^3$) and the ratios of OC/EC in PM_{2.5} on normal days, dust storms, and pollution events.

	NDs (n = 35)		DSs (n = 2)		HDs (n = 68)		BBs (n = 8)		FDs (n = 2)	
	Average	S.D.	Average	S.D.	Average	S.D.	Average	S.D.	Average	S.D.
OC	9.5	3.2	18.8	3.3	19.6	9.0	23.6	7.3	26.1	17.2
EC	4.1	1.2	6.0	1.5	10.6	5.8	6.2	2.0	9.5	6.8
TCA	19.4	5.9	36.1	6.7	41.9	19.4	43.9	12.9	51.2	34.3
OC/EC	2.3	0.6	3.2	0.3	2.0	0.6	4.0	1.1	2.8	0.1

NDs: normal days; DSs: dust storms; HDs: haze days; BBs: biomass-burning days; FDs: fireworks displays; OC: organic carbon; EC: elemental carbon; TCA: total carbonaceous aerosol ($1.6 \times \text{OC} + \text{EC}$); and S.D.: standard deviation.

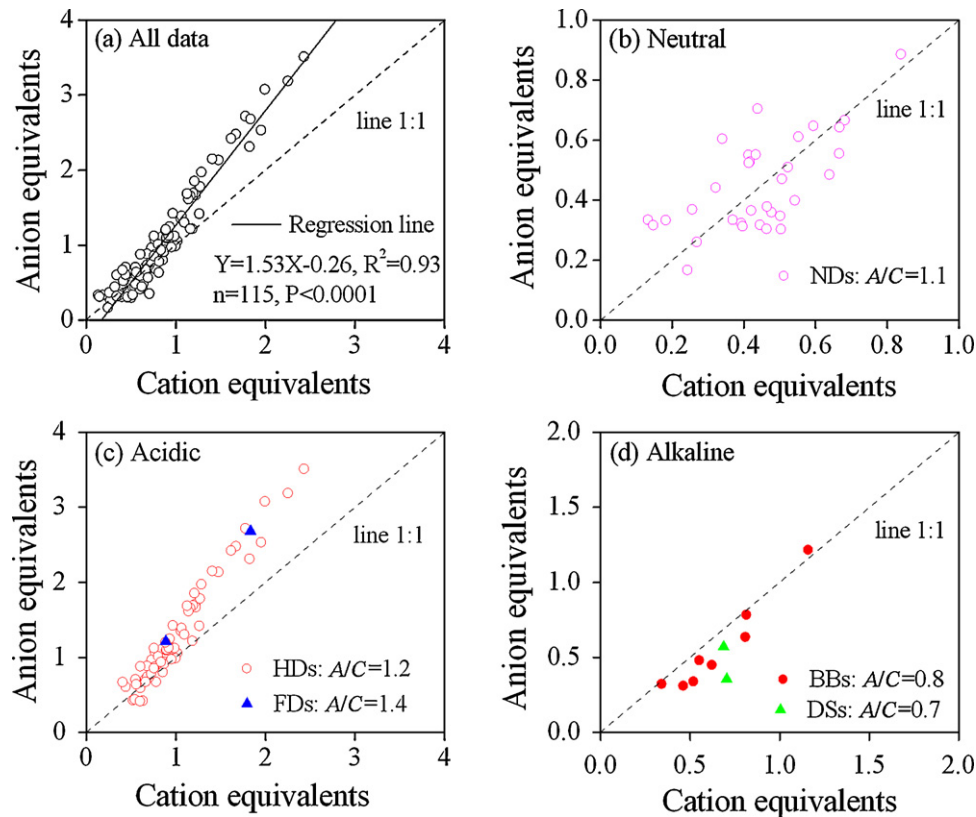


Fig. 4. Scatter plots of anion microequivalents versus cation microequivalents: (a) all samples, (b) neutral samples during normal days (NDs), (c) acidic samples during haze days (HDs) and fireworks displays (FDs), and (d) alkaline samples during dust storms (DSs) and biomass-burning days (BBs).

during NDs, while for HDs, BBs, and FDs, the concentrations were 2.1–2.7 times higher than that for NDs. Compared to the OC values, the EC concentrations were significantly lower, at 6.0, 10.6, 6.2, and 9.5 $\mu\text{g}/\text{m}^3$, accounting for 2.1%, 5.6%, 4.7%, and 4.5% of $\text{PM}_{2.5}$ mass for DSs, HDs, BBs, and FDs respectively.

Previously, the OC/EC ratio has been used to investigate emissions of carbonaceous aerosols (Cao et al., 2005, 2009; Han et al., 2008; Zhang et al., 2009). For example, the OC/EC ratio from biomass burning is substantially high, while fossil-fuel emissions tend to have low OC/EC ratios (Han, Cao, Lee, Ho, & An, 2010). Previous studies have determined OC/EC primary ratios of 9.0 for biomass burning (Cachier, Bremond, & Buat-Menard, 1989) and 1.1 for vehicle emissions (Watson, Chow, & Houck, 2001). As shown in Fig. 3, the highest OC/EC ratio was observed during a BB (4.0), whereas the lowest OC/EC ratio occurred during an HD (2.0), indicating the influence of vehicles.

Total carbonaceous aerosol (TCA) was calculated as the sum of organic matter ($\text{OM} = 1.6 \times \text{OC}$) and elemental carbon (Turpin & Lim, 2001). The average TCA concentrations during DSs, HDs, BBs, and FDs were 36.1, 41.9, 43.9, and 51.2 $\mu\text{g}/\text{m}^3$ respectively, accounting for 12.7%, 22.4%, 33.7%, and 24.1% of the $\text{PM}_{2.5}$ mass. Obviously, carbonaceous aerosol was one of the main components of pollution events, especially for BBs. As shown in Fig. 3, the concentration ratio of $\text{TCA}/\text{SO}_4^{2-}$ was greatest during BBs (3.6), followed by DSs (2.9), NDs (1.7), HDs (1.2), and FDs, the lowest (0.8). Consequently, the $\text{TCA}/\text{SO}_4^{2-}$ ratio may be useful for evaluating the contribution of biomass burning to aerosol loading.

3.5. Mass balance of $\text{PM}_{2.5}$ during four PM events

Fig. 5 illustrates the $\text{PM}_{2.5}$ mass balance for the major water-soluble ions, OM, EC, trace species, and soil dust during NDs, DSs,

and pollution events. Soil dust was estimated as $[\text{Al}]/0.08$, and trace species were calculated by summing all the elements and ions measured after subtracting the crustal matter (Al, Ti, Mn, and Fe) and the three secondary inorganic ions (NH_4^+ , SO_4^{2-} , and NO_3^-). As shown in Fig. 5, approximately 81.4%, 96.7%, 78.4%, 73.9%, and 94.3% of the $\text{PM}_{2.5}$ mass was explained by these seven components for NDs, DSs, HDs, BBs, and FDs respectively. During NDs, OM and SO_4^{2-} were the predominant fractions, accounting for 20.7% and 16.9%

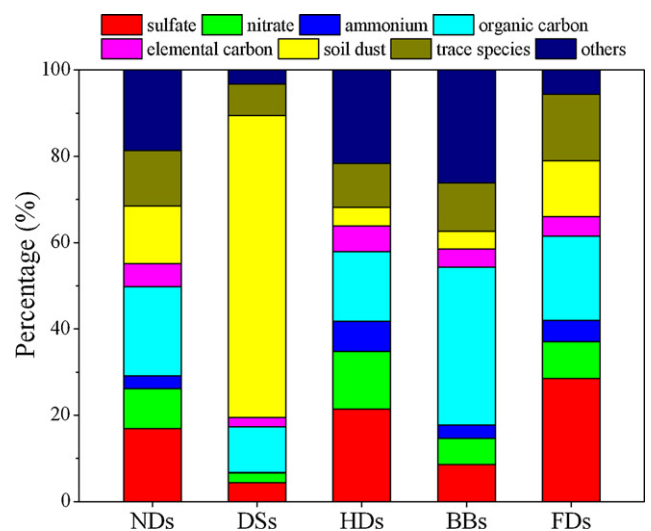


Fig. 5. Mass balance of chemical species in $\text{PM}_{2.5}$ during normal days (NDs), dust storms (DSs), haze days (HDs), biomass-burning days (BBs), and fireworks displays (FDs).

of the PM_{2.5} mass respectively, while other components made considerably smaller contributions, such as soil dust (13.3%) and NO₃⁻ (9.3%). For DS samples, soil dust was the largest contributor, accounting for 70.0% of PM_{2.5} mass, followed by OM (10.6%), SO₄²⁻ (4.4%), trace species (3.3%), NO₃⁻ (2.4%), and EC (2.1%). During HDs, SO₄²⁻ (21.5%) was the largest contributor to PM_{2.5}, followed by OM (16.2%), NO₃⁻ (13.3%), and trace species (10.2%). During BBs, OM (36.5%) was the largest contributor to PM_{2.5}, whereas other components contributed ~3–11%. During FDs, SO₄²⁻ (28.5%) was the largest contributor to PM_{2.5}, followed by OM (19.6%), trace species (15.3%), and soil dust (13.0%).

In this study, approximately 18.6%, 3.3%, 21.6%, 26.1%, and 5.7% of the PM_{2.5} mass was unidentified for ND, DS, HD, BB, and FD samples respectively. This may be due to uncertainties in chemical analysis, to underestimation of soil dust using [Al]/0.08, to the presence of undetermined organic acids in the PM_{2.5} samples, or to some combination of these.

4. Conclusions

In this study, daily fine particulate (PM_{2.5}) aerosol samples were collected in Chengdu from April 2009 to February 2010 to investigate the chemical characteristics of various pollution events. The PM_{2.5} mass was strongly elevated during all the pollution events. The concentrations of most elements during HDs were higher than during NDs, while enhanced dust elements concentrations were found during DSs. Ba, Sr, Cu, and Pb were enriched during FDs. The percentages of water-soluble ions varied for different types of pollution events; these discrepancies may be characteristic of the various emission sources. Enhanced levels of secondary inorganic ions (NH₄⁺, SO₄²⁻, and NO₃⁻) were found in HD and FD samples, while BBs and FDs were associated with high levels of K⁺. Low values of SO₄²⁻/K⁺ together with high values of TCA/SO₄²⁻ may be a tracer of BBs among all PM events, while low values of SO₄²⁻/K⁺ and TCA/SO₄²⁻ may be useful for distinguishing FDs from other PM events. Ion-balance calculations indicated that PM_{2.5} from HDs and FDs was more acidic than that from NDs, but that DS and BB particles were alkaline. The highest mass concentration of OC was found during FDs, while EC was most abundant during HDs. The highest OC/EC ratio was found during BBs and the lowest during HDs. Mass balance showed that organic matter, SO₄²⁻, and NO₃⁻ were the dominant chemical components during HDs, BBs, and FDs, while soil dust was highest during DSs.

Acknowledgments

This work was supported in part by projects from the Natural Science Foundation of China (NSFC40925009, 41230641), project from the “Strategic Priority Research Program” of the Chinese Academy of Sciences (Grant No. XDA05100401), and the Meteorological Innovative Research Project of Baoji Meteorological Bureau (No. T2012-01).

References

Andreae, M. O., Schmid, O., Yang, H., Chand, D., Zhen, Yu, J., et al. (2008). Optical properties and chemical composition of the atmospheric aerosol in urban Guangzhou, China. *Atmospheric Environment*, 42, 6335–6350.

Arimoto, R., Duce, R. A., Savoie, D. L., Prospero, J. M., Talbot, R., Cullen, J. D., et al. (1996). Relationships among aerosol constituents from Asia and the North Pacific during PEM-West A. *Journal of Geophysical Research*, 101, 2011–2023.

Cachier, H., Bremond, M. P., & Buat-Menard, P. (1989). Carbonaceous aerosols from different tropical biomass burning sources. *Nature*, 340, 371–373.

Cao, J. J., Chow, J. C., Watson, J. G., Wu, F., Han, Y. M., Jin, Z. D., et al. (2008). Size-differentiated source profiles for fugitive dust in the Chinese Loess Plateau. *Atmospheric Environment*, 42, 2261–2275.

Cao, J. J., Lee, S. C., Ho, K. F., Zhang, X. Y., Zou, S. C., Fung, K., et al. (2003). Characteristics of carbonaceous aerosol in Pearl River Delta Region, China during 2001 winter period. *Atmospheric Environment*, 37, 1451–1460.

Cao, J. J., Shen, Z. X., Chow, J. C., Qi, G. W., & Watson, J. G. (2009). Seasonal variations and sources of mass and chemical composition for PM₁₀ aerosol in Hangzhou, China. *Particology*, 7, 161–168.

Cao, J. J., Wang, Q. Y., Chow, J. C., Watson, J. G., Tie, X. X., Shen, Z. X., et al. (2012). Impacts of aerosol compositions on visibility impairment in Xi'an, China. *Atmospheric Environment*, 59, 559–566.

Cao, J. J., Wu, F., Chow, J. C., Lee, S. C., Li, Y., Chen, S. W., et al. (2005). Characterization and source apportionment of atmospheric organic and elemental carbon during fall and winter of 2003 in Xi'an, China. *Atmospheric Chemistry and Physics*, 5, 3127–3137.

Chang, D., Song, Y., & Liu, B. (2009). Visibility trends in six megacities in China 1973–2007. *Atmospheric Research*, 94, 161–167.

Che, H. Z., Zhang, X. Y., Li, Y., Zhou, Z. J., Qu, J. J., & Hao, X. J. (2009). Haze trends over the capital cities of 31 provinces in China, 1981–2005. *Theoretical and Applied Climatology*, 97, 235–242.

Chow, J. C., & Watson, J. G. (1999). Ion chromatography in elemental analysis of airborne particles. In S. Landsberger, & M. Creatchman (Eds.), *Elemental analysis of airborne particles* (pp. 97–137). Amsterdam: Gordon and Breach Science Publishers.

Chow, J. C., Watson, J. G., Chen, L. W. A., Chang, M. C. O., Robinson, N. F., Trimble, D., et al. (2007). The IMPROVE-A temperature protocol for thermal/optical carbon analysis: Maintaining consistency with a long-term database. *Journal of the Air & Waste Management Association*, 57, 1014–1023.

Chow, J. C., Watson, J. G., Robles, J., Wang, X., Chen, L. W. A., Trimble, D. L., et al. (2011). Quality assurance and quality control for thermal/optical analysis of aerosol samples for organic and elemental carbon. *Analytical and Bioanalytical Chemistry*, 401, 3141–3152.

de Kok, T. M. C. M., Driech, H. A. L., Hogervorst, J. G. F., & Briedé, J. J. (2006). Toxicological assessment of ambient and traffic-related particulate matter: A review of recent studies. *Mutation Research/Reviews in Mutation Research*, 613(2–3), 103–122.

Han, Y. M., Cao, J. J., Lee, S. C., Ho, K. F., & An, Z. S. (2010). Different characteristics of char and soot in the atmosphere and their ratio as an indicator for source identification in Xi'an, China. *Atmospheric Chemistry and Physics*, 10, 595–607.

Han, Y. M., Han, Z. W., Cao, J. J., Chow, J. C., Watson, J. G., An, Z. S., et al. (2008). Distribution and origin of carbonaceous aerosol over a rural high-mountain lake area Northern China and its transport significance. *Atmospheric Environment*, 42, 2405–2414.

Henriksson, S. V., Laaksonen, A., Kerminen, V. M., Räisänen, P., Järvinen, H., Sundström, A. M., et al. (2011). Spatial distributions and seasonal cycles of aerosols in India and China seen in global climate-aerosol model. *Atmospheric Chemistry and Physics*, 11, 7975–7990.

Husar, R. B., & Holloway, J. M. (1984). The properties and climate of atmospheric haze. In L. H. Ruhnke, & A. Deepak (Eds.), *Hygroscopic aerosols* (pp. 129–170). Hampton: A. Deepak Publishing.

Kim, K. H., Choi, G. H., Kang, C. H., Lee, J. H., Kim, J. Y., Youn, Y. H., et al. (2003). The chemical composition of fine and coarse particles in relation with the Asian Dust events. *Atmospheric Environment*, 37, 753–765.

Lee, K. H., Kim, Y. J., & Kim, M. J. (2006). Characteristics of aerosol observed during two severe haze events over Korea in June and October 2004. *Atmospheric Environment*, 40, 5146–5155.

Ning, Z., & Sioutas, C. (2010). Atmospheric processes influencing aerosols generated by combustion and the inference of their impact on public exposure: A review. *Aerosol and Air Quality Research*, 10, 43–58.

Pope, C. A., Burnett, R. T., Thun, M. J., Calle, E. E., Krewski, D., Ito, K., et al. (2002). Lung cancer, cardiopulmonary mortality, and long-term exposure to fine particulate air pollution. *JAMA: The Journal of the American Medical Association*, 287, 1132–1141.

Shen, Z. X., Arimoto, R., Cao, J. J., Zhang, R. J., Li, X. X., Du, N., et al. (2008). Seasonal variations and evidence for the effectiveness of pollution controls on water-soluble inorganic species in total suspended particulates and fine particulate matter from Xi'an, China. *Journal of the Air & Waste Management Association*, 58, 1560–1570.

Shen, Z. X., Cao, J. J., Arimoto, R., Han, Y. M., Zhu, C. S., Tian, J., et al. (2010). Chemical characteristics of fine particles (PM₁) from Xi'an, China. *Aerosol Science and Technology*, 44, 461–472.

Shen, Z. X., Cao, J. J., Arimoto, R., Han, Z. W., Zhang, R. J., Han, Y. M., et al. (2009). Ionic composition of TSP and PM_{2.5} during dust storms and air pollution episodes at Xi'an, China. *Atmospheric Environment*, 43, 2911–2918.

Shen, Z. X., Cao, J. J., Arimoto, R., Zhang, R. J., Jie, D. M., Liu, S. X., et al. (2007). Chemical composition and source characterization of spring aerosol over Horqin sand land in northeastern China. *Journal of Geophysical Research*, 112, D14315.

Shen, Z. X., Wang, X., Zhang, R. J., Ho, K. F., Cao, J. J., & Zhang, M. G. (2011). Chemical composition of water-soluble ions and carbonate estimation in spring aerosol at a semi-arid site of Tongyu, China. *Aerosol and Air Quality Research*, 11, 360–368.

Shi, G. L., Zeng, F., Li, X., Feng, Y. C., Wang, Y. Q., Liu, G. X., et al. (2011). Estimated contributions and uncertainties of PCA/MLR-CMB results: Source apportionment for synthetic and ambient datasets. *Atmospheric Environment*, 45, 2811–2819.

- Tan, J. H., Duan, J. C., Chen, D. H., Wang, X. H., Guo, S. J., Bi, X. H., et al. (2009). Chemical characteristics of haze during summer and winter in Guangzhou. *Atmospheric Research*, *94*, 238–245.
- Tian, H., Wang, Y., Xue, Z., Cheng, K., Qu, Y., Chai, F., et al. (2010). Trend and characteristics of atmospheric emissions of Hg, As, and Se from coal combustion in China, 1980–2007. *Atmospheric Chemistry and Physics*, *10*, 11905–11919.
- Tie, X. X., Brasseur, G. P., Zhao, C. S., Granier, C., Massie, S., Qin, Y., et al. (2006). Chemical characterization of air pollution in Eastern China and the Eastern United States. *Atmospheric Environment*, *40*, 2607–2625.
- Torigoe, K., Hasegawa, S., Numata, O., Yazaki, S., Matsunaga, M., Boku, N., et al. (2000). Influence of emission from rice straw burning on bronchial asthma in children. *Pediatrics International*, *42*, 143–150.
- Turpin, B. J., & Lim, H. J. (2001). Species contributions to PM_{2.5} mass concentrations: Revisiting common assumptions for estimating organic mass. *Aerosol Science and Technology*, *35*, 602–610.
- Vecchi, R., Bernardoni, V., Cricchio, D., D'Alessandro, A., Fermo, P., Lucarelli, F., et al. (2008). The impact of fireworks on airborne particles. *Atmospheric Environment*, *42*, 1121–1132.
- Wang, S., Yuan, W., & Shang, K. (2006). The impacts of different kinds of dust events on PM₁₀ pollution in northern China. *Atmospheric Environment*, *40*, 7975–7982.
- Wang, Y., Zhuang, G., Xu, C., & An, Z. (2007). The air pollution caused by the burning of fireworks during the lantern festival in Beijing. *Atmospheric Environment*, *41*, 417–431.
- Wang, Y., Zhuang, G. S., Tang, A. H., Yuan, H., Sun, Y. L., Chen, S., et al. (2005). The ion chemistry and the source of PM_{2.5} aerosol in Beijing. *Atmospheric Environment*, *39*, 3771–3784.
- Watson, J. G. (2002). Visibility: Science and regulation. *Journal of the Air & Waste Management Association*, *52*, 628–713.
- Watson, J. G., Chow, J. C., & Houck, J. E. (2001). PM_{2.5} chemical source profiles for vehicle exhaust, vegetative burning, geological material, and coal burning in Northwestern Colorado during 1995. *Chemosphere*, *43*, 1141–1151.
- Xu, L., Chen, X., Chen, J., Zhang, F., He, C., Zhao, J., et al. (2012). Seasonal variations and chemical compositions of PM_{2.5} aerosol in the urban area of Fuzhou, China. *Atmospheric Research*, *104–105*, 264–272.
- Ye, B. M., Ji, X. L., Yang, H. Z., Yao, X. H., Chan, C. K., Cadle, S. H., et al. (2003). Concentration and chemical composition of PM_{2.5} in Shanghai for a 1-year period. *Atmospheric Environment*, *37*, 499–510.
- Zhang, R. J., Ho, K. F., Cao, J. J., Han, Z., Zhang, M., Cheng, Y., et al. (2009). Organic carbon and elemental carbon associated with PM₁₀ in Beijing during spring time. *Journal of Hazardous Materials*, *172*, 970–977.